



Frost, Ray L. and Bahfenne, Silmarilly (2009) *Raman and mid-IR spectroscopic study of the magnesium carbonate minerals– brugnatellite and coalingite*. Journal of Raman Spectroscopy, 40(4). pp. 360-365.

© Copyright 2009 John Wiley & Sons

1 **Raman and mid-IR spectroscopic study of the magnesium carbonate minerals–**
2 **brugnatellite and coalingite**

3
4 **Ray L. Frost • and Silmarilly Bahfenne**

5
6 Inorganic Materials Research Program, School of Physical and Chemical
7 Sciences, Queensland University of Technology, GPO Box 2434, Brisbane
8 Queensland 4001, Australia.

9
10 **Abstract**

11
12 **Two hydrated hydroxy magnesium carbonate minerals brugnatellite**
13 **and coalingite with a hydrotalcite-like structure have been studied by**
14 **Raman spectroscopy. Intense bands are observed at 1094 cm⁻¹ for**
15 **brugnatellite and at 1093 cm⁻¹ for coalingite attributed CO₃²⁻ v₁**
16 **symmetric stretching mode. Additional low intensity bands are**
17 **observed at 1064 cm⁻¹. The existence of two symmetric stretching modes**
18 **is accounted for in terms of different anion structural arrangements.**
19 **Very low intensity bands at 1377 and 1451 cm⁻¹ is observed for**
20 **brugnatellite and the Raman spectrum of coalingite displays two bands**
21 **at 1420 and 1465 cm⁻¹ attributed to the (CO₃)²⁻ v₃ antisymmetric**
22 **stretching modes. Very low intensity bands at 792 cm⁻¹ for brugnatellite**
23 **and 797 cm⁻¹ for coalingite are assigned to the CO₃²⁻ out-of-plane bend**
24 **(v₂).**

25 **X-ray diffraction studies by other researchers have shown these**
26 **minerals are disordered. This is reflected in the difficulty of obtaining**
27 **Raman spectra of reasonable quality and explains why the Raman**
28 **spectra of these minerals have not been previously or sufficiently**
29 **described. A comparison is made with the Raman spectra of other**
30 **hydrated magnesium carbonate minerals.**

31

• Author to whom correspondence should be addressed (r.frost@qut.edu.au)

32 **KEYWORDS:** Sequestration of greenhouse gases; Magnesium Carbonate; $(\text{CO}_3)^{2-}$;
33 brugnatellite, coalingite, artinite; dypingite; Raman spectroscopy

34 INTRODUCTION

35

36

37 The ability to be able to easily and readily detect minerals is of importance,^{1,2}
38 especially so where carbonate minerals are concerned. The technique of infrared
39 spectroscopy does meet these requirements. What is not known is that many
40 carbonate-containing minerals especially the secondary minerals are soluble and can
41 translocate. The proposal to remove greenhouse gases by pumping CO_2 several
42 kilometres below the ground implies that many carbonate containing minerals will be
43 formed. Two such minerals are the ferric ion-bearing minerals coalingite
44 $\text{Mg}_{10}\text{Fe}_2^{3+}(\text{CO}_3)(\text{OH})_{24}\cdot 2\text{H}_2\text{O}$ ³⁻¹⁰ and brugnatellite $\text{Mg}_6\text{Fe}^{3+}(\text{CO}_3)(\text{OH})_{13}\cdot 4\text{H}_2\text{O}$ ^{8,11-15}.
45 The formulae of these minerals appear to be related to that of hydrotalcites. Pastor-
46 Rodriguez and Taylor reported the crystal structure of coalingite and presented a
47 model coalingite with a $d(003)$ spacing of 1.25 nm¹⁰. Brugnatellite is related to the
48 manasseite and pyroaurite mineral group whereas coalingite is related to
49 hydromagnesite and pyroaurite mineral group. Fundamental knowledge of these two
50 minerals is lacking. Pumping greenhouse gases into magnesium-bearing mineral
51 deposits is likely to result in the formation of these types of minerals.

52

53

54 Vibrational spectroscopy has proven very useful for the study of minerals¹⁶⁻²¹.
55 Indeed, Raman spectroscopy has also proven to be very useful for the study of
56 diagenetically related minerals as often occurs with many carbonate minerals²²⁻³¹.
57 Some previous studies have been undertaken by the authors, using Raman
58 spectroscopy to study complex secondary minerals formed by crystallisation from
59 concentrated sulphate solutions. This paper reports the detection and structural
60 analysis of two magnesium carbonate minerals namely brugnatellite and coalingite
61 using Raman spectroscopy complimented with infrared spectroscopy. The application
62 of this work is important for the understanding of the geosequestration of greenhouses
63 gases and the consequential detection of carbonate bearing minerals.

64

65

66 **EXPERIMENTAL**

67 **Minerals**

68

69 The origin of the minerals is as follows: Brugnatellite - Monte, Ramazzo,
70 Genoa, Liguria, Italy; Brugnatellite - Higasi-Kuroda-Guchi, Inasa-Cho, Inasa-Gun,
71 Aichi Prefecture, Japan; Coalingite - Union Carbide Mine, Southern San Benito
72 County, California. The minerals are associated with iron-containing brucite.

73

74 **Raman microprobe spectroscopy**

75

76 The crystals of halogenated carbonates were placed and oriented on the stage
77 of an Olympus BHSM microscope, equipped with 10x and 50x objectives and part of
78 a Renishaw 1000 Raman microscope system, which also includes a monochromator, a
79 filter system and a Charge Coupled Device (CCD). Raman spectra were excited by a
80 HeNe laser (633 nm) at a nominal resolution of 2 cm^{-1} in the range between 100 and
81 4000 cm^{-1} . The laser power at the sample is less than 5 mW. Exposure time was 20
82 seconds with 64 accumulations. Spectra were calibrated using the 520.5 cm^{-1} line of a
83 silicon wafer. Previous studies by the authors provide more details of the experimental
84 technique.

85 **Mid-IR spectroscopy**

86 Infrared spectra were obtained using a Nicolet Nexus 870 FTIR spectrometer
87 with a smart endurance single bounce diamond ATR cell. Spectra over the $4000\text{--}525$
88 cm^{-1} range were obtained by the co-addition of 64 scans with a resolution of 4 cm^{-1}
89 and a mirror velocity of 0.6329 cm/s . Spectra were co-added to improve the signal to
90 noise ratio. The infrared spectra are displayed in the Supplementary Information.

91 Spectral manipulation such as baseline adjustment, smoothing and normalisation
92 were performed using the Spectracalc software package GRAMS (Galactic Industries
93 Corporation, NH, USA). Band component analysis was undertaken using the Jandel
94 'Peakfit' software package which enabled the type of fitting function to be selected

95 and allows specific parameters to be fixed or varied accordingly. Band fitting was
96 done using a Lorentz-Gauss cross-product function with the minimum number of
97 component bands used for the fitting process. The Gauss-Lorentz ratio was
98 maintained at values greater than 0.7 and fitting was undertaken until reproducible
99 results were obtained with squared correlations of r^2 greater than 0.995.

100

101

102 **RESULTS AND DISCUSSION**

103

104 **Spectroscopy of the carbonate anion**

105

106 Nakamoto *et al.* first published and tabulated the selection rules for unidentate
107 and bidentate anions including the carbonate anion³². The free ion, CO_3^{2-} with D_{3h}
108 symmetry exhibits four normal vibrational modes; a symmetric stretching vibration
109 (ν_1), an out-of-plane bend (ν_2), a doubly degenerate asymmetric stretch (ν_3) and
110 another doubly degenerate bending mode (ν_4). The symmetries of these modes are A_1'
111 (R) + A_2'' (IR) + E' (R, IR) + E'' (R, IR) and occur at 1063, 879, 1415 and 680 cm^{-1}
112 respectively. Generally, strong Raman modes appear around 1100 cm^{-1} due to the
113 symmetric stretching vibration (ν_1), of the carbonate groups, while intense IR and
114 weak Raman peaks near 1400 cm^{-1} are due to the asymmetric stretch (ν_3). Infrared
115 modes near 800 cm^{-1} are derived from the out-of-plane bend (ν_2). Infrared and Raman
116 modes around 700 cm^{-1} region are due to the in-plane bending mode (ν_4). This mode
117 is doubly degenerate for undistorted CO_3^{2-} groups³². As the carbonate groups become
118 distorted from regular planar symmetry, this mode splits into two components³².
119 Infrared and Raman spectroscopy provide sensitive test for structural distortion of
120 CO_3^{2-} .

121

122 **Raman Spectroscopy**

123

124 The complete Raman spectra of brugnatellite and coalingite across the full
125 wavenumber range showing the relative intensities of bands in the Raman spectra are
126 provided in supplementary information Fig.1S and 2S. The Raman spectra of the two
127 brugnatellite minerals and the coalingite mineral in the 550 to 1250 cm^{-1} range are

128 shown in Figs 1 and 2, respectively. The infrared spectrum of the two brugnatellite
129 minerals in the 525 to 1600 cm^{-1} region is provided in the supplementary material
130 Figure 3S. An intense band at 1094 cm^{-1} for the Aichi brugnatellite is assigned to the
131 CO_3^{2-} ν_1 symmetric stretching mode. A second band is also observed at 1064 cm^{-1}
132 and is also assigned to this vibrational mode. The formula of brugnatellite is
133 $\text{Mg}_6\text{Fe}^{3+}(\text{CO}_3)(\text{OH})_{13}\cdot 4\text{H}_2\text{O}$ and possesses a hydrotalcite type structure. Thus the
134 CO_3^{2-} anion may be bonded to both the divalent and trivalent cations. This in itself
135 may lead to two symmetric stretching vibrations. An alternative explanation for the
136 peak at 1064 cm^{-1} may be ascribed to carbonate anions in the hydrotalcite interlayer.
137 For the Monte brugnatellite, the two bands at 1087 and 1102 cm^{-1} are assigned to the
138 CO_3^{2-} ν_1 symmetric stretching mode. It is interesting that the CO_3^{2-} band positions are
139 different for the two brugnatellite minerals. This is understandable in terms of a
140 hydrotalcite structure where different anion structural arrangements will occur. The
141 Raman spectrum of the mineral coalingite also shows an extremely intense band at
142 1093 cm^{-1} with a low intensity band at 1065 cm^{-1} .

143

144 The Raman band at 938 cm^{-1} (Aichi) and 959 cm^{-1} (Monte) are attributed to
145 OH deformation modes from the MgOH and FeOH units. The intensity of this band
146 is intense in the infrared spectrum but low in the Raman spectrum; for MgOH and
147 FeOH units there is a very large change in dipole moment but a poor scattering cross
148 section. Two very low intensity bands are observed at 890 and 928 cm^{-1} for
149 coalingite. Farmer also commented on the difficulty of obtaining Raman spectra for
150 hydrated and hydrated hydroxy carbonate magnesium minerals and commented that
151 the internal modes of the internal CO_3^{2-} vibrations are either broadened or not
152 observed. Two infrared bands are observed at 952 and 990 cm^{-1} for brugnatellite
153 (Aichi) and 955 and 1017 cm^{-1} for brugnatellite (Monte). The corresponding infrared
154 bands in the coalingite spectrum are observed at 951 and 1011 cm^{-1} . The infrared
155 spectrum of the coalingite mineral in the 525 to 1600 cm^{-1} region is provided in the
156 supplementary material Figure 4S. One possible assignment of these bands is to the
157 OH deformation modes of the MgOH units and the FeOH units. The ratio of the
158 intensity of the bands implies that the higher wavenumber band is due to FeOH units
159 and the lower wavenumber band to the MgOH units.

160

161 A very weak Raman band is observed at 792 cm^{-1} for Aichi brugnatellite and
162 765 cm^{-1} for Monte brugnatellite and is assigned to the CO_3^{2-} out-of-plane bend (ν_2).
163 In the Raman spectrum of artinite as reported by Farmer a low intensity band at 810
164 cm^{-1} for artinite may be assigned to this vibration. In the Raman spectrum of
165 coalingite two Raman bands are observed at 702 and 797 cm^{-1} and are assigned to the
166 $(\text{CO}_3)^{2-}$ ν_2 bending modes. The observations reported here are in harmony with
167 Farmer's commentary. Coleyshaw *et al.* also did not find any intensity of bands in
168 this position for the Raman spectra of lansfordite and nesquehonite. These authors
169 reported the infrared spectra of CO_3^{2-} out-of-plane bend (ν_2) as 854 cm^{-1} . In the
170 Raman spectra of artinite a reasonably intense band at around 700 cm^{-1} is assigned to
171 the CO_3^{2-} ν_2 in-plane bend. Only a single band is observed for artinite whereas two
172 bands are found for dypingite at 725 and 760 cm^{-1} . Farmer in the Raman spectrum of
173 artinite reported two bands for this vibrational mode at 693 and 704 cm^{-1} ³³.
174 Coleyshaw *et al.* reported bands at 698 and 774 cm^{-1} for synthetic lansfordite, 705 and
175 771 cm^{-1} for natural nesquehonite and 713 and 781 cm^{-1} for synthetic nesquehonite ³⁴.
176 For the Yoshikawaite dypingite infrared spectrum low intensity bands are observed at
177 755 and 799 cm^{-1} . For the Aichi artinite these bands are found at 722 and 762 cm^{-1} .
178 These bands are assigned to the $(\text{CO}_3)^{2-}$ ν_4 bending modes. The observation of more
179 than one band supports the concept that there are multiple $(\text{CO}_3)^{2-}$ bending modes as a
180 result of the distortion of the $(\text{CO}_3)^{2-}$ units in the dypingite and artinite structures.

181

182 The Raman spectra of brugnatellite in the 1250 to 1750 cm^{-1} region and of
183 coalingite in the $1250 - 2500\text{ cm}^{-1}$ region are displayed in Figs 3 and 4 respectively.
184 Very low intensity bands at 1377 and 1451 cm^{-1} is observed for the Aichi
185 brugnatellite and two very low intensity bands at 1323 and 1591 cm^{-1} for the Monte
186 brugnatellite. The infrared spectrum of brugnatellite (Aichi) bands is observed at
187 1342 , 1401 and 1443 cm^{-1} and for brugnatellite (Monte) at 1330 , 1383 and 1400 cm^{-1} .
188 The Raman spectrum of coalingite displays two bands at 1420 and 1465 cm^{-1} . These
189 bands are attributed to the $(\text{CO}_3)^{2-}$ antisymmetric stretching modes. In the infrared
190 spectrum of coalingite the antisymmetric $(\text{CO}_3)^{2-}$ stretching modes are observed at
191 1372 and 1404 cm^{-1} . A comparison may be made with the Raman spectrum of other
192 hydrated hydroxy magnesium carbonates such as dypingite and artinite in this spectral
193 region. For the Yoshikawaite dypingite Raman bands are observed at 1366 , 1447 and
194 1524 cm^{-1} and at 1365 and 1527 cm^{-1} for Clear Creek dypingite. These bands are

195 assigned to CO_3^{2-} ν_3 antisymmetric stretching vibrations. These bands were not
196 observed in the Raman spectrum of artinite as reported by Farmer³³. Based upon
197 infrared spectra, Farmer reported ν_3 bands for artinite at 1320, 1355 and 1440 cm^{-1} .
198 No infrared bands were provided for dypingite by Farmer and no vibrational spectra
199 are readily available. Coleyshaw *et al.* published results for the ν_3 bands for
200 lansfordite and nesquehonite³⁴. Raman bands for synthetic lansfordite were found at
201 1424 and 1514 cm^{-1} and for synthetic nesquehonite at 1423 and 1516 cm^{-1} ³⁴. Even
202 though these bands are of very low intensity in the Raman spectrum, the bands are of
203 high intensity in the infrared spectrum. The $(\text{CO}_3)^{2-}$ symmetric stretching mode is
204 complimented with the antisymmetric stretching modes found in the 1300 to 1450 cm^{-1}
205 region where a series of overlapping infrared bands are observed providing a
206 complex spectral infrared profile. For artinite the infrared $(\text{CO}_3)^{2-}$ antisymmetric
207 stretching modes are observed at 1325, 1381, 1439 cm^{-1} (Aichi) and 1376, 1441, 1535
208 cm^{-1} (Clear Creek). For the dypingite from Clear Creek, these $(\text{CO}_3)^{2-}$ anti symmetric
209 stretching bands are observed at 1312, 1438, 1534 and 1585 cm^{-1} . These bands appear
210 better defined for the Yoshikawaite dypingite with clearly resolved bands at 1380,
211 1405, 1479 1509
212 cm^{-1} .

213
214 The low intensity Raman band observed at 1657 cm^{-1} is assigned to the water
215 δ bending mode. This band is normally strongly infrared active and very weakly
216 Raman active if observed at all. The position of this band provides evidence of
217 strongly hydrogen bonded water in the brugnatellite mineral structure. Weakly or non-
218 hydrogen bonded water, is normally observed at around 1595 cm^{-1} as may be found in
219 the infrared spectrum of water vapour. For liquid water the water bending vibration is
220 found at 1630 cm^{-1} . Two bands are observed for coalingite at 1655 and 1768 cm^{-1} .
221 These bands provide evidence for water molecules being very strongly hydrogen
222 bonded in the coalingite structure. The Raman data may be compared with the
223 infrared results which are significantly more intense. The probable assignment of
224 these bands is to the water HOH bending mode. The fact that two bands are observed
225 suggests that there are two types of water present in the brugnatellite structure. The
226 band at 1592 cm^{-1} is attributed to non-hydrogen bonded water and corresponds to the
227 position of the water bending mode of water vapour, whereas the band at 1646 cm^{-1}
228 corresponds to strongly hydrogen bonded water. The coalingite infrared spectrum

229 shows two bands at 1595 and 1681 cm^{-1} . This later band shows that the water is very
230 strongly hydrogen bonded and corresponds to the water stretching vibration at 2943
231 cm^{-1} whereas the 1595 cm^{-1} band is reflected in the OH stretching region by the band
232 at 3337 cm^{-1} .

233

234

235 The Raman spectra of brugnatellite in the 2800 to 4000 cm^{-1} region and of
236 coalingite in the 2500 – 4000 cm^{-1} region are shown in Figs 5 and 6. The infrared
237 spectrum of the two brugnatellite minerals in the 2700 to 3800 cm^{-1} region are
238 provided in the supplementary material Figure 5S and the infrared spectra of
239 coalingite in the 2700 to 3800 cm^{-1} region in Figure 6S. The Raman spectrum of
240 brugnatellite in this spectral region is characterised by two sets of bands: (a) an
241 intense band at 3594 cm^{-1} (Aichi) and 3696 cm^{-1} (Monte) assigned to the MgOH and
242 FeOH stretching vibrations and (b) the broad profile of overlapping bands at 3030 and
243 3227 cm^{-1} attributed to water stretching vibrations. Raman bands of lower intensity
244 are observed at 3697 and 3642 cm^{-1} which are also assigned to MgOH/ FeOH
245 stretching bands. The range of OH stretching bands suggests that MgOH and FeOH
246 units are not all equivalent in the brugnatellite structure. For coalingite, sharp Raman
247 bands are observed at 3585, 3596 and 3632 cm^{-1} and are also assigned to MgOH/
248 FeOH stretching bands.

249

250 CONCLUSIONS

251

252 The understanding of the chemistry of hydrated magnesium minerals including
253 brugnatellite and coalingite including their spectroscopy and thermal stability is of
254 extreme importance from the standpoint of geosequestration which involves the
255 pumping of green house gases to significant depths below the surface of the earth.
256 Such a process, it is hoped, would involve the formation of many carbonate minerals.
257 The high partial pressure of CO_2 is significant in that many different types of
258 carbonates will be formed. Of significance are the magnesium carbonate minerals
259 which will be formed by reaction of the liquefied CO_2 with magnesium minerals such
260 as brucite and periclase. Among these minerals there is the possibility of the

261 formation of brugnatellite and coalingite which are hydrotalcite-like in structure and
262 may be formed over a reasonable wide temperature range.

263

264 Published X-ray diffraction studies show the minerals brugnatellite and
265 coalingite are disordered. This is reflected in the difficulty of obtaining spectra of
266 reasonable quality and explains why the Raman spectra of these minerals have not
267 been previously or sufficiently described. Raman spectroscopy has been used to
268 characterise the two magnesium bearing minerals brugnatellite and coalingite and the
269 bands related to the mineral structure. The minerals are characterised by CO_3^{2-} ν_1
270 symmetric stretching modes but very weak antisymmetric stretching and bending
271 modes. These bands proved difficult to detect.

272

273

274 **Acknowledgments**

275

276 The financial and infra-structure support of the Queensland University of Technology,
277 Inorganic Materials Research Program is gratefully acknowledged. The Australian
278 Research Council (ARC) is thanked for funding the instrumentation. Mr Dermot
279 Henry of Museum Victoria is thanked for the loan of the minerals.

280 **References**

281

- 282 1. Hunt, GR, Ashley, RP. *Econ. Geol.* 1979; **74**: 1613.
- 283 2. Hunt, GR, Evarts, RC. *Geophys.* 1981; **46**: 316.
- 284 3. Caillere, S. *Compt. rend.* 1944; **219**: 256.
- 285 4. Delnavaz, H, Allmann, R. *Zeit.r Krist.* 1988; **183**: 175.
- 286 5. Frondel, C. *Am. Min.* 1941; **26**: 295.
- 287 6. Ivanov, OK. *Materialy po Mineral. Mestorozhd. Urala, Sverdlovsk* 1984: 75.
- 288 7. Jambor, JL. *Am. Min.* 1969; **54**: 437.
- 289 8. Kolmer, H, Postl, W. *Mitteilung.* 1977; **45**: 137.
- 290 9. Mumpton, FA, Jaffe, HW, Thompson, CS. *Am. Min.* 1965; **50**: 1893.
- 291 10. Pastor-Rodriguez, J, Taylor, HFW. *Min. Mag.* 1971; **38**: 286.
- 292 11. Artini, E. *Atti della Accademia Nazionale dei Lincei*, 1910; **18**: 3.
- 293 12. Caillere, S. *Bull. Soc. Franc, Mineral.* 1943; **66**: 494.
- 294 13. Fenoglio, M. *Rev. Geol.* 1938; **19**: 128.
- 295 14. Grey, IE, Ragozzini, R. *J. Solid State Chem.* 1991; **94**: 244.
- 296 15. Taylor, HFW. *Min. Mag.* 1969; **37**: 338.
- 297 16. Frost, RL, Cejka, J, Ayoko, G. *J. Raman. Spectrosc.* 2008; **39**: 495.
- 298 17. Frost, RL, Cejka, J, Ayoko, GA, Dickfos, MJ. *J. Raman. Spectrosc.* 2008; **39**:
- 299 374.
- 300 18. Frost, RL, Dickfos, MJ, Cejka, J. *J. Raman. Spectrosc.* 2008; **39**: 582.
- 301 19. Frost, RL, Hales, MC, Wain, DL. *J. Raman. Spectrosc.* 2008; **39**: 108.
- 302 20. Frost, RL, Keeffe, EC. *J. Raman. Spectrosc.* 2008; **in press**.
- 303 21. Palmer, SJ, Frost, RL, Ayoko, G, Nguyen, T. *J. Raman. Spectrosc.* 2008; **39**:
- 304 395.
- 305 22. Frost, RL, Bouzaid, JM. *J. Raman. Spectrosc.* 2007; **38**: 873.
- 306 23. Frost, RL, Bouzaid, JM, Martens, WN, Reddy, BJ. *J. Raman. Spectrosc.* 2007;
- 307 **38**: 135.
- 308 24. Frost, RL, Cejka, J. *J. Raman. Spectrosc.* 2007; **38**: 1488.
- 309 25. Frost, RL, Cejka, J, Ayoko, GA, Weier, ML. *J. Raman. Spectrosc.* 2007; **38**:
- 310 1311.
- 311 26. Frost, RL, Cejka, J, Weier, ML. *J. Raman. Spectrosc.* 2007; **38**: 460.
- 312 27. Frost, RL, Cejka, J, Weier, ML, Martens, WN, Ayoko, GA. *J. Raman.*
- 313 *Spectrosc.* 2007; **38**: 398.

- 314 28. Frost, RL, Dickfos, MJ. *J. Raman. Spectrosc.* 2007; **38**: 1516.
- 315 29. Frost, RL, Palmer, SJ, Bouzaid, JM, Reddy, BJ. *J. Raman. Spectrosc.* 2007;
316 **38**: 68.
- 317 30. Frost, RL, Pinto, C. *J. Raman. Spectrosc.* 2007; **38**: 841.
- 318 31. Frost, RL, Weier, ML, Williams, PA, Leverett, P, Kloprogge, JT. *J. Raman.*
319 *Spectrosc.* 2007; **38**: 574.
- 320 32. Nakamoto, K, Fujita, J, Tanaka, S, Kobayashi, M. *J. Am. Chem. Soc.* 1957;
321 **79**: 4904.
- 322 33. Farmer, VC *Mineralogical Society Monograph 4: The Infrared Spectra of*
323 *Minerals*, 1974.
- 324 34. Coleyshaw Esther, E, Crump, G, Griffith William, P. *Spectrochim. Acta A*,
325 2003; **59**: 2231.
- 326
- 327
- 328
- 329

330 **List of Figures**

331

332 Fig. 1 Raman spectra of brugnatellite from Monte and Aichi Prefecture in the 550 to
333 1250 cm^{-1} region.

334

335 Fig. 2 Raman spectra of coalingite in the 550 to 1250 cm^{-1} region.

336

337 Fig. 3 Raman spectra of brugnatellite from Monte and Aichi Prefecture in the 1250 to
338 1750 cm^{-1} region.

339

340 Fig. 4 Raman spectra of coalingite in the 1250 to 2500 cm^{-1} region.

341

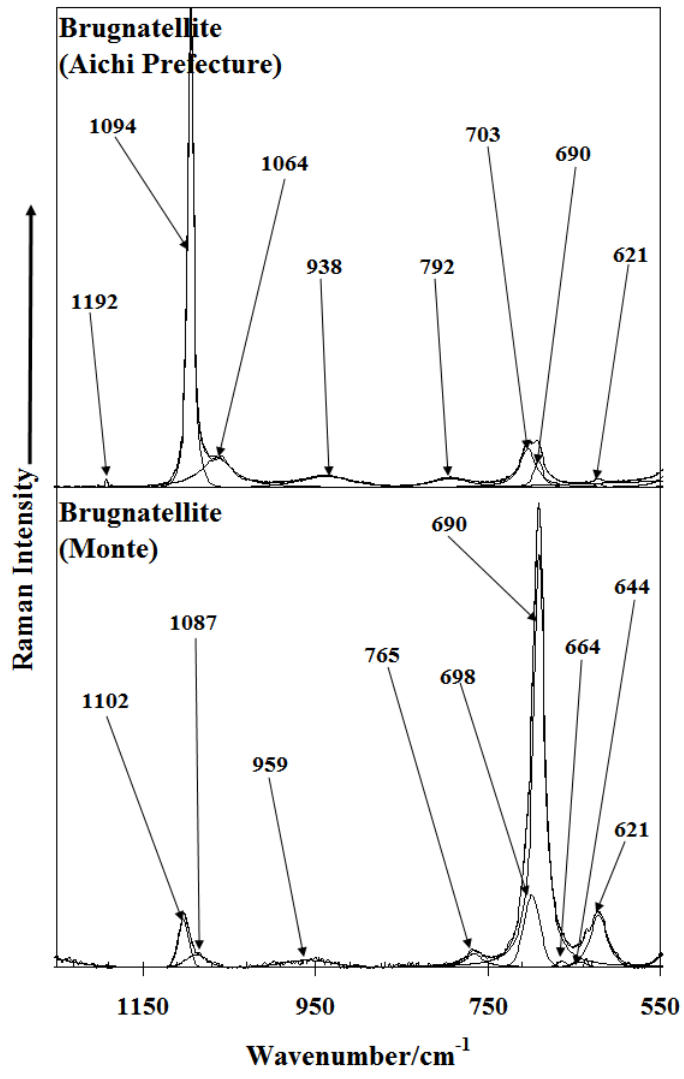
342 Fig. 5 Raman spectra of brugnatellite from Monte and Aichi Prefecture in the 2800 to
343 4000 cm^{-1} region.

344

345 Fig. 6 Raman spectra of coalingite in the 2500 to 4000 cm^{-1} region.

346

347



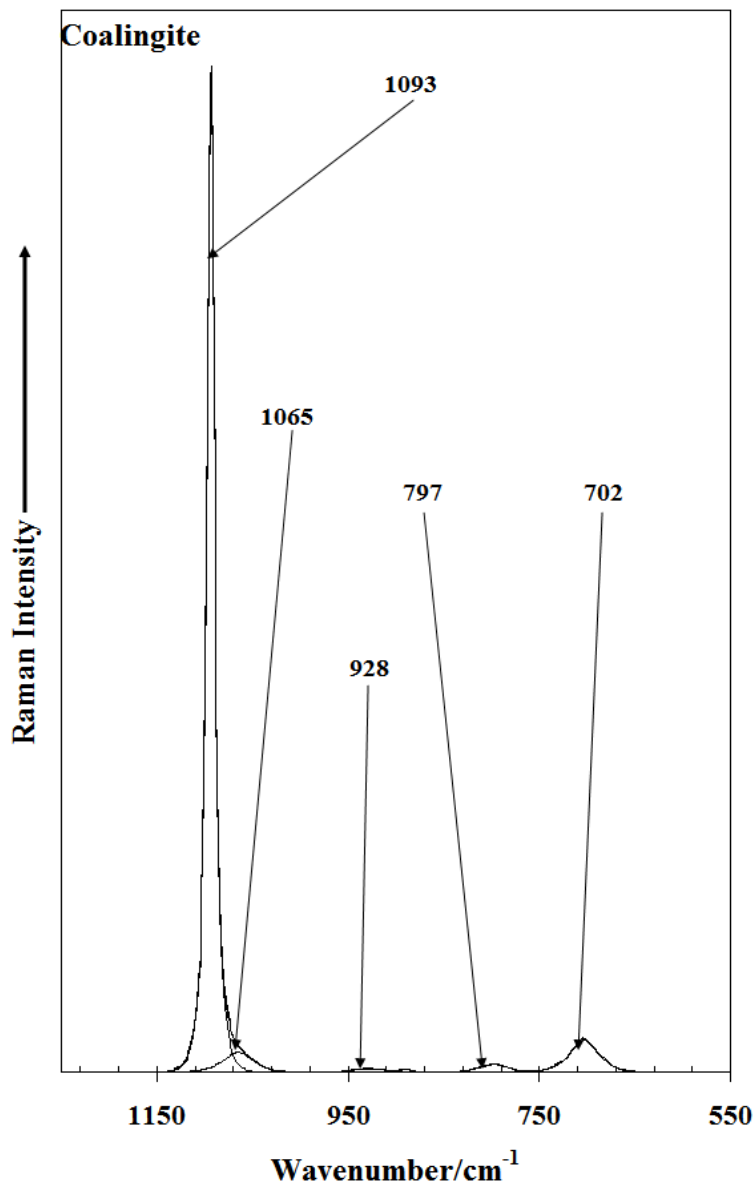
348

349

350 **Fig 1**

351

352



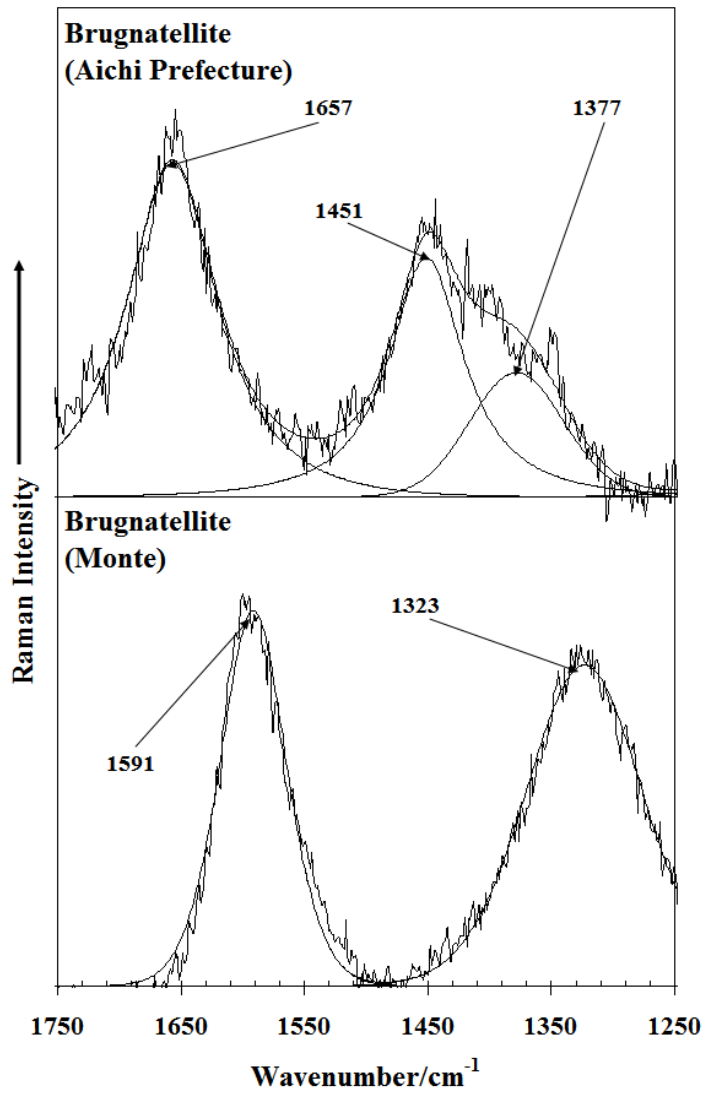
353

354

355 **Fig 2**

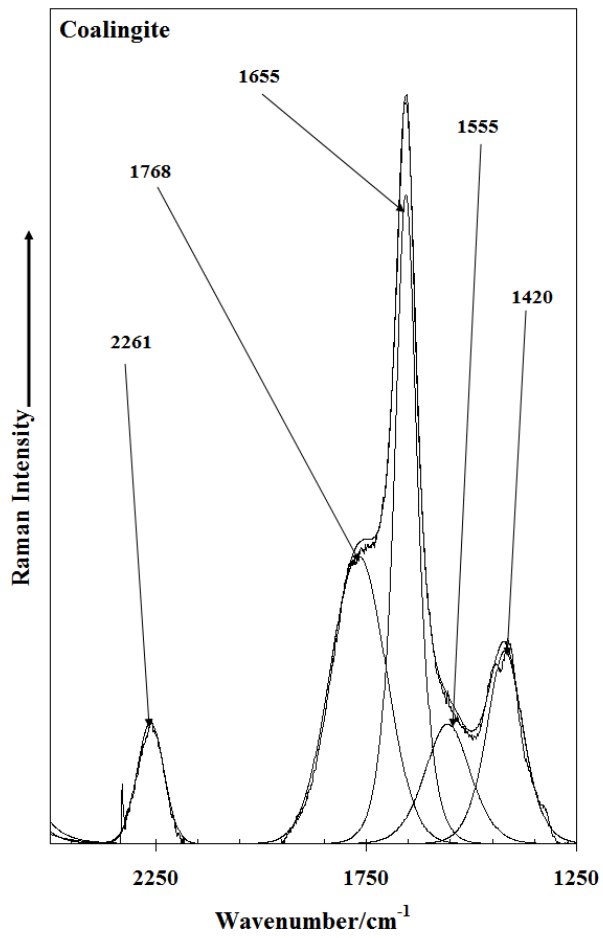
356

357



358
359
360
361
362

Fig 3



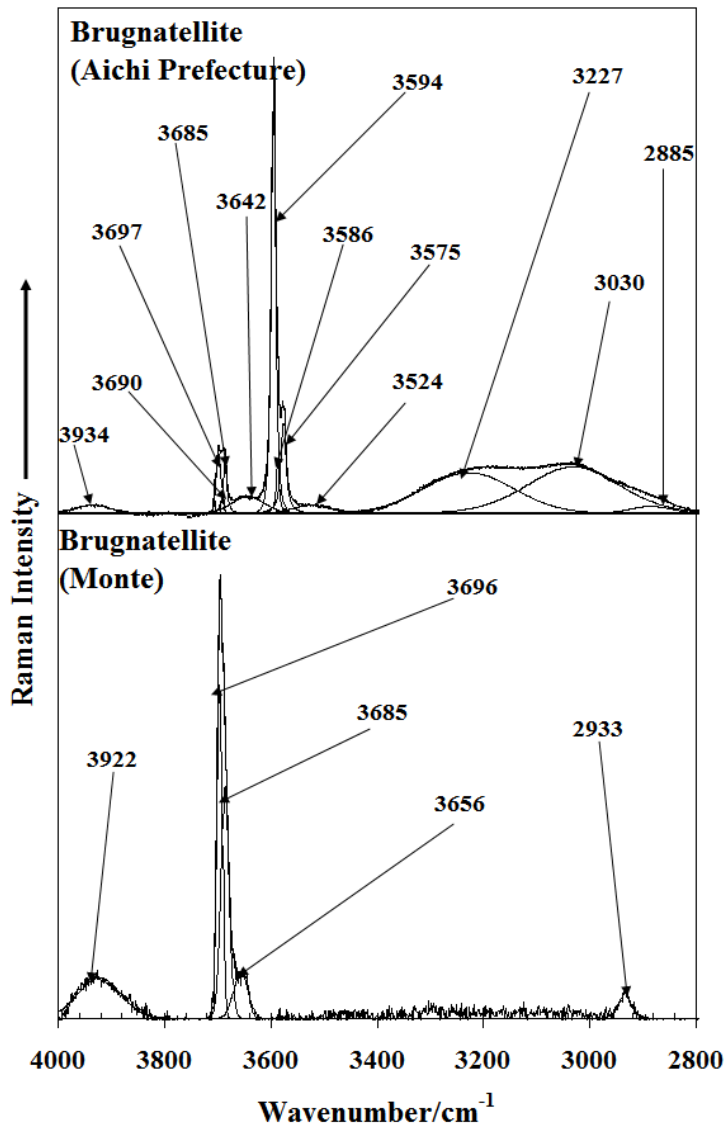
363

364

365 **Fig 4**

366

367



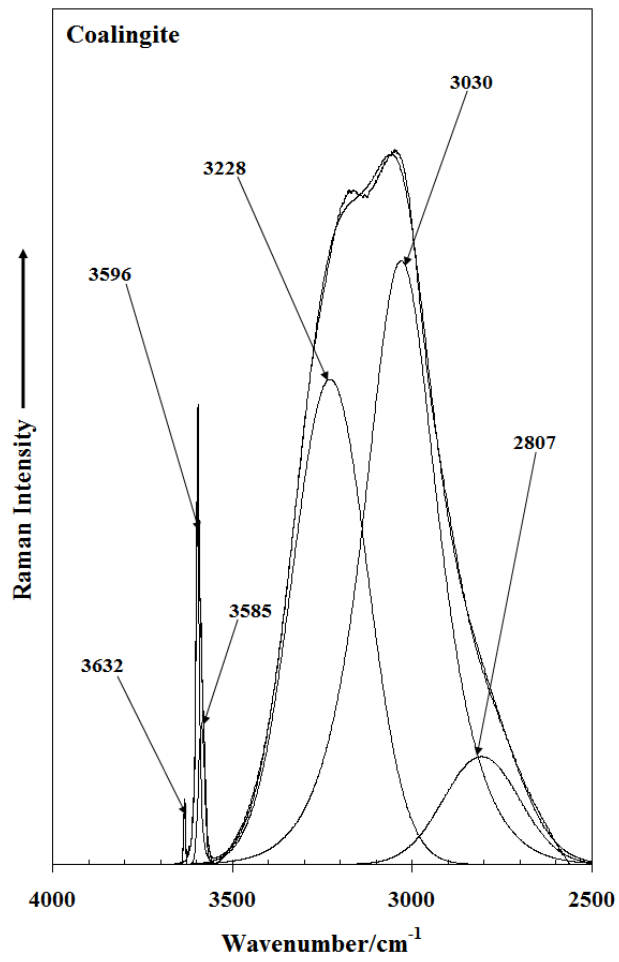
368

369

370 **Fig 5**

371

372



373

374

375 **Fig 6**